

# Multi-side kinetic modeling of <sup>13</sup>C metabolic MR using [1-<sup>13</sup>C]pyruvate

Pedro A Gómez Damian<sup>1,2</sup>, Jonathan I Sperl<sup>1</sup>, Oleksandr Khagai<sup>1</sup>, Stefan Grott<sup>1</sup>, Eliane Weidl<sup>3</sup>, Martin A Janich<sup>3</sup>, Florian Wiesinger<sup>1</sup>, Steffen J Glaser<sup>4</sup>, Axel Haase<sup>5</sup>, Markus Schwaiger<sup>3</sup>, Rolf F Schulte<sup>1</sup>, and Marion I Menzel<sup>1</sup>

<sup>1</sup>GE Global Research, Munich, Germany, <sup>2</sup>Tecnológico de Monterrey, Monterrey, Mexico, <sup>3</sup>Nuclear Medicine, Technische Universität München, Munich, Germany, <sup>4</sup>Department Chemie, Technische Universität München, Munich, Germany, <sup>5</sup>IMETUM, Technische Universität München, Munich, Germany

## Introduction

Hyperpolarized <sup>13</sup>C metabolic imaging allows real-time in-vivo measurements of metabolic conversion. Experiments are performed by polarization of [1-<sup>13</sup>C]pyruvate with dynamic nuclear polarization and subsequent rapid dissolution, producing a hyperpolarized liquid suitable for intravenous injection[1]. In a previous study [2] we examined the metabolic exchange between [1-<sup>13</sup>C]pyruvate and its downstream metabolites [1-<sup>13</sup>C]alanine, [1-<sup>13</sup>C]lactate, [1-<sup>13</sup>C]pyruvate hydrate and [1-<sup>13</sup>C]bicarbonate in male Wistar rats by acquiring slice-selective FID signals in slices dominated by heart, liver, and kidney tissue. Using pyruvate doses of 0.1 – 0.4 mmol/kg (body mass), we examined the effect of transient exposure to high pyruvate blood concentrations, causing potential saturation of cellular uptake and metabolic conversion, semi-quantitatively using signal-time integrals [2]. Further quantification of metabolite conversion can be achieved through kinetic modeling of time-domain signals. Present kinetic models, i.e. two-side integral (2SIM) [3] or two-side differential (2SDM) [4] represent a two-side interaction between pyruvate and one specific downstream metabolite. Since pyruvate interacts dynamically and simultaneously with all of the downstream metabolites, the purpose of this work is the implementation of a multi-side, dynamic model involving all possible biochemical pathways. It was validated by comparing it to kinetic modeling obtained with two-side integral and two-side differential models.

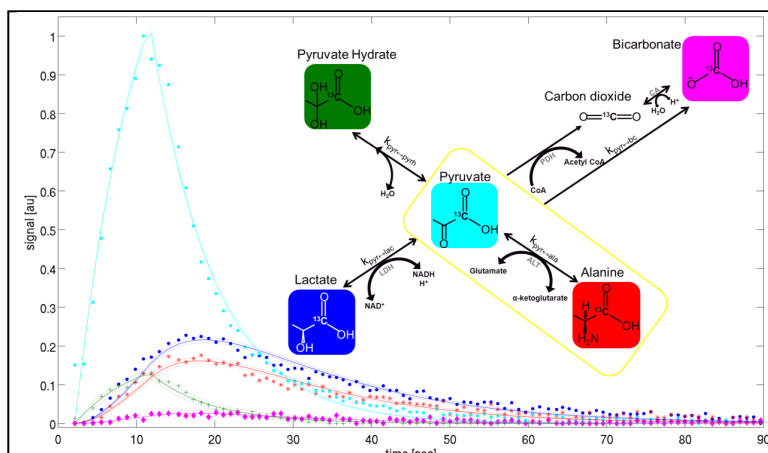


Fig 1: Schematic representation of all possible metabolic pathways taken by [1-<sup>13</sup>C]pyruvate (LDH = lactate dehydrogenase, ALT = alanine transaminase, PDC = pyruvate dehydrogenase complex, CA = carbonic anhydrase) and metabolic time fit of data acquired for a 0.4 mmol/kg dose in kidney predominant tissue. The yellow square represents the two-side exchange kinetic model, in this case between [1-<sup>13</sup>C]pyruvate and [1-<sup>13</sup>C]alanine. The proposed model takes into account not only this single pyruvate-to-metabolite exchange, but includes all of the metabolites represented in the diagram.

## Theory and Methods:

Kinetic modeling parameters were determined by fitting the multi-side model (MSIM) to time-domain dynamic data (see Fig. 1). The model consists of a series of exponential equations similar to [3], but takes into account all of the metabolites into a one-step fitting process, which also models the input functions for  $I_{pyr}$  and rapid chemical conversion to pyruvate hydrate ( $I_{pyrh}$ ) as follows:

$$M_{pyr}(t) = \begin{cases} \frac{I_{pyr}}{R_{pyr}}(1 - e^{-R_{pyr}(t-t_{arrival})}), & t_{arrival} \leq t < t_{end} \\ \frac{M_{pyr}(t_{end})}{R_{pyr}}e^{-R_{pyr}(t-t_{end})}, & t \geq t_{end}. \end{cases} \quad \text{with}$$

$$R_{pyr} = r_{pyr} + \sum_x k_{pyr \rightarrow x}$$

$$M_x(t) = \begin{cases} \frac{k_{pyr \rightarrow x} I_{pyr}}{R_{pyr} - r_x} \left( \frac{1 - e^{-r_x(t-t_{arrival})}}{r_x} - \frac{1 - e^{-R_{pyr}(t-t_{arrival})}}{R_{pyr}} \right), & t_{arrival} \leq t < t_{end} \\ \frac{M_{pyr}(t_{end}) k_{pyr \rightarrow x}}{R_{pyr} - r_x} (e^{-r_x(t-t_{end})} - e^{-R_{pyr}(t-t_{end})}) + M_x(t_{end}) e^{-r_x(t-t_{end})}, & t \geq t_{end}. \end{cases}$$

$$M_{pyrh}(t) = \begin{cases} \frac{k_{pyr \rightarrow pyrh} I_{pyr}}{R_{pyr} - r_{pyrh}} \left( \frac{1 - e^{-r_{pyrh}(t-t_{arrival})}}{r_{pyrh}} - \frac{1 - e^{-R_{pyr}(t-t_{arrival})}}{R_{pyr}} \right) + \frac{I_{pyrh}}{r_{pyrh}} (1 - e^{-r_{pyrh}(t-t_{arrival})}), & t_{arrival} \leq t < t_{end} \\ \frac{M_{pyr}(t_{end}) k_{pyr \rightarrow pyrh}}{R_{pyr} - r_{pyrh}} (e^{-r_{pyrh}(t-t_{end})} - e^{-R_{pyr}(t-t_{end})}) + M_{pyrh}(t_{end}) e^{-r_{pyrh}(t-t_{end})}, & t \geq t_{end} \end{cases}$$

The fitting was done in a least-squares sense and involved the gradient calculation of the parameters. Parameter values were compared with values of both two-side models (data not shown) and for different pyruvate doses and evaluated for statistically significant differences comparing the different doses of pyruvate injection.

## Results and Conclusion:

The model presented was shown to be robust and have an optimal convergence point. In comparison to the two-side exchange models, the multi-side model yielded smaller pyruvate-to-metabolite exchange rates and improved determination of T1 values for pyruvate. Dose effects observed in [2] were confirmed and quantified through pyruvate-to-metabolite exchange rate values (data not shown). The proposed kinetic modeling method that takes into account all of the downstream metabolites in one system can be used for the quantification of pyruvate metabolic exchange rates. Parameter interdependency allowed a more accurate quantification than other modeling methods and can therefore be useful for the monitoring of metabolic activity in different tissues, which is reflected in a reduced noise bias.

## Acknowledgements:

BMBF grant numbers 01EZ0826/7, 01EZ1114A/B. The authors take responsibility for the content of the publication. PAGD acknowledges German DAAD, Modality of Professional Experience (MEP), Tecnológico de Monterrey.

## References:

- [1] Ardenkjaer-Larsen JH, 2003, PNAS, 100, 10158-10163.; [2] Janich MA, 2011, NMR Biomed in press; [3] Zierhut ML, 2010, J Magn Reson, 202, 85-92; [4] Wiesinger F, 2010, ISMRM, p. 3282.

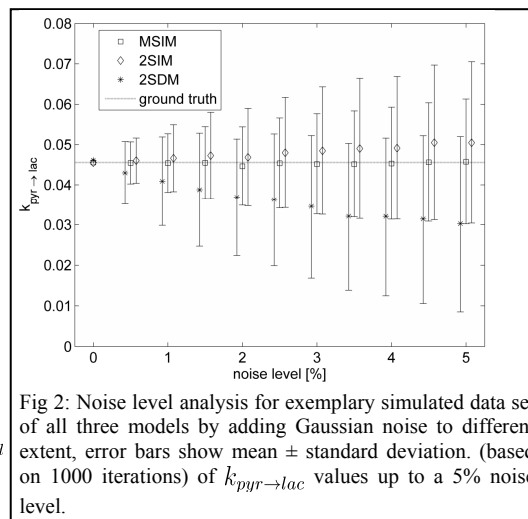


Fig 2: Noise level analysis for exemplary simulated data set of all three models by adding Gaussian noise to different extent, error bars show mean ± standard deviation. (based on 1000 iterations) of  $k_{pyr \rightarrow lac}$  values up to a 5% noise level.